Available online at www.sciencedirect.com
SCIENCE DIRECT
Catalysis Today 101 (2005) 389–395
CATALYSIS TODAY
www.elsevier.com/locate/cattod

# Vis and UV photocatalytic detoxification methods (using $TiO_2$, $TiO_2/H_2O_2$, $TiO_2/O_3$, $TiO_2/S_2O_8^{2-}$, $O_3$, $H_2O_2$, $S_2O_8^{2-}$, $Fe^{3+}/H_2O_2$ and $Fe^{3+}/H_2O_2/C_2O_4^{2-}$) for dyes treatment

Joaquín R. Domínguez *, Jesús Beltrán, Oscar Rodríguez

*Departamento de Ingeniería Química y Energética, Facultad de Ciencias, Universidad de Extremadura (UEx), Avda. de Elvas, s/n. E-06071, Badajoz, Spain*

Available online 23 March 2005

**Abstract**

The degradation of Acid Red 88 azo dye in water was investigated in laboratory-scale experiments using 21 oxidation processes. Colour, COD and TOC removals were evaluated for each oxidation system. The processes were studied in three groups: processes deriving from the heterogeneous photocatalysis (using $TiO_2$), oxidation systems based on Fenton-type reactions (homogeneous photocatalysis) and processes based on the application of ozone (ozone catalysis). The results obtained showed that the decolourization rate was quite different for each oxidation process. After 15 min reaction time the relative decolourization order established was: $H_2O_2$ = vis < $H_2O_2/Fe^{3+}$/vis < $TiO_2/H_2O_2$/vis = $TiO_2$/vis < UV < UV/$S_2O_8^{2-}$ < $H_2O_2/Fe^{3+}/C_2O_4^{2-}$/vis < $H_2O_2$/UV < $H_2O_2/Fe^{3+}$/UV < $TiO_2/S_2O_8^{2-}$/UV < $TiO_2$/UV = $TiO_2/H_2O_2$/UV < $O_3$ < $O_3/H_2O_2$ < $O_3/H_2O_2$/UV < $O_3$/UV = $O_3$/vis < $O_3/H_2O_2$/UV/$Fe^{3+}$ < $O_3/TiO_2$/vis < $O_3/TiO_2$. Nevertheless, taking into account the mineralization of the compound (measured as TOC and COD removal) at the end of the experiment, the order was slightly different. For example, the photo-Fenton-ozone process ($O_3/H_2O_2$/UV/$Fe^{3+}$) seems to be more appropriate than $O_3/TiO_2$. Also, in a kinetic study, the pseudo-first-order kinetic rate was determined for each oxidation system. This overall constant was split up into two components: direct oxidation by irradiation (photolysis) and oxidation by free radicals (mainly $HO^{\bullet}$).


*Keywords:* Advanced oxidation processes; Titanium dioxide; Ozone; Azo dye; Acid Red 88; Photo-Fenton

## 1. Introduction

Dyes have been used widely in the textile industry, photographic industry, coating industry and photochemical applications. Since the discovery of synthetic fibers, the use of disperse dyes has been continuously increased in the textile industry. Disperse azo dyes, in particular, cause environmental concern due to their widespread use, their degradation products, such as toxic aromatic amines, and their low removal rate during aerobic waste treatment [1].

For the removal of such recalcitrant pollutant, traditional physical techniques (coagulation, adsorption on activated carbon, reverse osmosis and ultrafiltration, etc.) can generally be used [2]. Nevertheless, these methods are usually non-destructive, and the post-treatment of the adsorbent materials or solid wastes is necessary and expensive [3]. Advanced oxidation is one of the potential alternatives to decolourize and to reduce recalcitrant wastewater loads from textile dyeing and finishing effluents. This process implies generation and subsequent reaction of radicals, mainly hydroxyl radicals, which are the most powerful oxidizing species after fluorine [4]. Among AOPs, treatment with ozone or Fenton-type processes have proven to yield very good results either for complete mineralization of reactive dyes [5].

Ozone decomposition into $HO^{\bullet}$ can be activated via $OH^-$, $H_2O_2$, short UV light ($\lambda < 360$ nm) and reduced transition metals [6,7]. Combinations like $O_3$/UV, $O_3/H_2O_2$ and $O_3/OH^-$ have been studied for the treatment of various organic compounds found in water and industrial wastewater [8,9]. More recently, ozonation processes catalyzed by transition metals have been investigated for the degradation of organic pollutants [10,11].

* Corresponding author. Tel.: +34 924 289385; fax: +34 924 289385.
*E-mail address:* jrdoming@unex.es (J.R. Domínguez).

0920-5861/$ – see front matter 
doi:10.1016/j.cattod.2005.03.010

Transition metals such as iron and manganese or titanium have been applied in the form of their solutions. Fenton's reagent and related reactions combine iron compounds with hydrogen peroxide or other peroxides to bring about the oxidation of organic compounds. Fenton-like reactions have been applied to the oxidation of organic pollutants in water. The photoassisted Fenton's reaction with light in the near-UV to visible region is especially powerful for treating wastewater and often leads to extensive mineralization of the target pollutant. In the past decade, considerable attention has focused on using nanocrystalline $TiO_2$ as a photocatalyst for the degradation of organic pollutants [12–14]. Several papers have discussed the fundamentals of the photocatalytic degradation process [15,16]. The photocatalyst, titanium dioxide, is a wide bandgap (3.2 eV) semiconductor, corresponding to radiation in the near-UV range. Upon the absorption of this UV energy, $TiO_2$ particles will form a paired electron ($e^-$) and hole ($h^+$), in the conduction band and valence band. The positive hole is apparently able to oxidize a water molecule to hydroxyl radical. The hydroxyl radical, in turn, is a powerful oxidant. Moreover, the possible use of vis-light has recently drawn attention. Some authors [17] demonstrated how the photobleaching dyes could be achieved by sunlight irradiation using $TiO_2$ as photocatalyst.

On the other hand, the Acid Red 88 is an azo dye very common in a great variety of applications. It was therefore chosen as a representative azo dye to comparatively study its degradation by 21 oxidation methods. The objectives were to provide data about the degree of removal, to report values of the kinetic rate constants for the global processes, and to compare the efficiency of the different advanced oxidation methods. Also, the increases obtained in the degradation levels due to the presence of combined oxidations compared to the single oxidation processes were determined, and the partial contribution of the radical pathway to the global oxidation process.

## 2. Experimental

### 2.1. Materials

Acid Red 88 azo dye (4-(2-hydroxy-1-naphthylazo)-1-naphthalenesulfonic acid, C.I. 15620) was obtained from Aldrich. Hydrogen peroxide (33% w/v), sodium oxalate and ferrous sulfate heptahydrate from Merck. Titanium dioxide (Degussa P-25) from Degussa Portugal; average diameter, BET surface area, and density of $TiO_2$ particles were 20 nm, 50 $m^2/g$, and 3.90 $g/cm^3$ at 20 °C, respectively. This supposes a ratio of surface area to volume of the photoreactor of $2.5 \times 10^4$ $m^{-1}$.

### 2.2. Ozonation

Ozone was generated from dried oxygen by an ozone generator "Sander Labor Ozonisator: mod. 300.5" of the company Erwin Sander. The ozone concentration was determined by an ozone measuring device model "Quant Ozone BG" (Erwin Sander Elektroapparatebau). Ozonation was performed in the reactor by bubbling the ozone/air mixture in the solution, at a volume stream of 40 l/h through a sintered glass filter fixed at the bottom of the reactor. For all the experiments, the ozone partial pressure at the input to the reactor was kept constant at 0.16 kPa.

### 2.3. Photoreactor

The reactor consisted of a 500 ml glass cylinder provided with the necessary elements (inlets for stirring, sampling, bubbling the gas feed in the ozonation experiments, venting and measuring the temperature) for the development of the different processes: photodecomposition, photo-Fenton, ozonation and the different combinations of these oxidants. The radiation source was located axially, held in a quartz sleeve. An external water jacket surrounded the reactor in order to maintain a constant temperature of 293 K. The UV-radiation source was an "Heraeus TNN-15W" low pressure mercury vapour lamp which emits $2.0 \times 10^{-6}$ Eins/s. The vis-radiation source was a halogen lamp "Philips Capsuleline Pro-50W" (936 cd/sr) immersed in an UV-block glass. Both lamps were located axially, held in a quartz sleeve. In the experiments with hydrogen peroxide, the concentration was $5.40 \times 10^{-4}$ M. The reaction volume was 350 ml in all cases and the initial concentration of the dye was $1.35 \times 10^{-4}$ M. In experiments with the presence of iron, the concentration was in all cases 10 times less than that of $H_2O_2$, which is the optimal ratio according to our experience [18].

Aqueous solutions containing 50 mg/l azo dye were prepared with ultrapure water (conductivity of 0.058 mS/cm) from a Millipore Waters Milli-Q purification unit. Decolourization capacity was determined by absorbance measurements at the maximum visible absorbance wavelength of 505 nm. The so-prepared aqueous solution had a concentration of 0.135 mM and was characterised by COD equal to 70.5 mg $O_2$/l and TOC = 23.06 mg C/l.

### 2.4. Analyses

The kinetic study was supported on the decolourisation of the azo dye. Samples of the reaction medium were withdrawn at regular intervals and analyzed for UV–Vis-absorbance. The optical absorption of azo dye solution was determined, at 505 nm, and recorded by a Unicam UV–Vis spectrophotometer. The concentration of the unconverted dye in solution was defined as the dye absorption maximum by Eq. (1), and the translucent colour value (TCV) was defined by Eq. (2):

$$\frac{C_A}{C_A^0} \times 100 = \frac{TCV}{TCV_0} \times 100 \quad (1)$$

$$TCV = A_\lambda 1000 d^{-1} \quad (2)$$

where $A_\lambda$ is the spectral absorbance and $d$ the length of the quartz cell (10 mm).

Final chemical oxygen demand (COD) and total organic carbon (TOC) were also measured. These two parameters were done using commercially available test kits from Dr. Lange (Germany).

## 3. Results and discussion

The first stage was to compare the 21 oxidation processes applied to the oxidation of the azo dye. For this, oxidation processes were ranked from lesser to greater efficacy, according to the levels of decolourization attained at 15 min. The resulting efficacy ranking is as follows:

$$\begin{aligned}H_2O_2 &= \text{vis} < H_2O_2/Fe^{3+}/\text{vis} < TiO_2/H_2O_2/\text{vis}\\ &= TiO_2/\text{vis} < \text{UV} < \text{UV}/S_2O_8^{2-} < H_2O_2/Fe^{3+}/C_2O_4^{2-}\\ &\quad /\text{vis} < H_2O_2/\text{UV} < H_2O_2/Fe^{3+}/\text{UV} < TiO_2/\\ &\quad S_2O_8^{2-}/\text{UV} < TiO_2/\text{UV} = TiO_2/H_2O_2/\text{UV}\\ &\quad < O_3 < O_3/H_2O_2 < O_3/H_2O_2/\text{UV} < O_3/\text{UV}\\ &= O_3/\text{vis} < O_3/H_2O_2/\text{UV}/Fe^{3+} < O_3/TiO_2/\text{vis}\\ &\quad < O_3/TiO_2.\end{aligned}$$

As a first approximation and to compare the different processes, the overall reaction process is taken to consist of four contributions: direct oxidation by UV or vis irradiation (photolysis), direct oxidation by $H_2O_2$, direct oxidation by ozone (ozonation), and oxidation by free radicals (mainly $HO^\bullet$):

$$P + h\nu \xrightarrow{k_P} P_{ox} \quad (3)$$

$$P + HO^\bullet \xrightarrow{k_R} P_{ox} \quad (4)$$

$$P + H_2O_2 \xrightarrow{k_H} P_{ox} \quad (5)$$

$$P + O_3 \xrightarrow{k_{O_3}} P_{ox} \quad (6)$$

With respect to direct oxidation of the compound by hydrogen peroxide and vis-irradiation, this was found experimentally not to exist. It also has to be noted that, at the reaction pH (pH 7), ozone is decomposed (Eqs. (7)–(9)) and reacts with the compound via free radicals [19].

$$O_3 + OH^- \rightarrow O_3^{\bullet -} + HO^\bullet \quad (7)$$

$$O_3^{\bullet -} \rightarrow O_2 + O^{\bullet -} \quad (8)$$

$$O^{\bullet -} + H^+ \rightarrow HO^\bullet \quad (9)$$

It will also be assumed that the first reaction (UV-photolysis) will take place whenever they form part of the combined oxidation system. This assumption is based on the fact that in combined oxidation systems (binaries, ternaries, etc.) in which UV radiation is involved, only a minimal part of the emitted radiation is consumed in generating free radicals. In accord with this reaction scheme, the overall process rate can be written as the sum of two processes: direct photolysis ($r_P$) and free radical reaction ($r_R$):

$$-r_T = \left[-\frac{dC_P}{dt}\right] = -(r_P + r_R) \quad (10)$$

$$(k_P + k_R)C_P = kC_P \quad (11)$$

In order to study further the improvements provided by the different AOPs, the different oxidation systems are divided into three groups: processes deriving from the heterogeneous photocatalysis (using $TiO_2$), systems based on Fenton-type reactions (homogeneous photocatalysis) and processes based on the application of ozone (ozone catalysis).

### 3.1. Heterogeneous photocatalysis

Photoexcitation with light of an energy greater than the $TiO_2$ band gap promotes an electron from the valence band to the conduction band, and leaves an electronic vacancy or hole ($h^+$) in the valence band. Thus the act of photoexcitation generates an electron–hole pair:

$$TiO_2 + h\nu \rightarrow TiO_2(h^+ + e^-) \quad (12)$$

$$TiO_2(h^+ + e^-) \rightarrow TiO_2 \quad (13)$$

In order to achieve chemically productive photocatalysis, electron–hole pair recombination must be suppressed. This can be achieved by "trapping" these species with the surface adsorbates. The photo-excited electrons are trapped by molecular oxygen. In this case, as the solution is saturated with oxygen, the reaction (13) must be negligible:

$$e^- + O_2(\text{ads.}) \rightarrow O_2^-(\text{ads.}) \quad (14)$$

The main hole traps are adsorbed water molecules and $OH^-$ ions [20,21] producing $HO^\bullet$ radicals. Eq. (18) represents the possible oxidation by positive holes. At this pH (pH 7) the

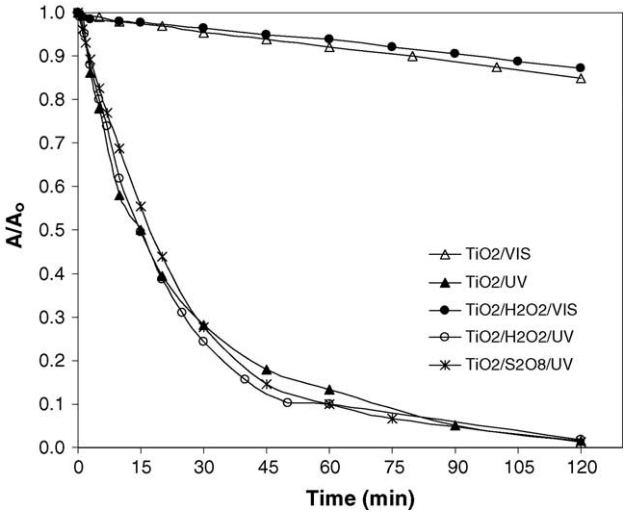


Fig. 1. Disappearance curves of dye in the group of experiments based on $TiO_2$.

Table 1
Rate constants and mineralization obtained at 2 h. Heterogeneous photocatalysis

| System | Colour removal at 15 min (%) | $k \times 100$ ($min^{-1}$) | $k_R \times 100$ ($min^{-1}$) | RR (%) | COD removal[a] (%) | TOC removal[a] (%) | $\varepsilon_c^0$ |
|---|---|---|---|---|---|---|---|
| $TiO_2$/vis | 2.5 | 0.13 | 0.13 | 99 | 0–5 | 0–5 | −1.9 |
| $TiO_2$/UV | 47 | 3.36 | 3.19 | 95 | 53 | 38 | −0.4 |
| $TiO_2/H_2O_2$/vis | 2.5 | 0.10 | 0.10 | 99 | 7 | 9 | −2.0 |
| $TiO_2/H_2O_2$/UV | 50 | 4.63 | 4.46 | 96 | 57 | 40 | −0.2 |
| $TiO_2/S_2O_8^{2-}$/UV | 48 | 3.70 | 3.53 | 95 | 46 | 61 | −1.9 |

$\varepsilon_c^0$: final oxidation state of residual carbon.
[a] Results obtained at 2 h of reaction.

reaction of the positive hole with the hydroxide ions must be favoured (Eq. (16)):

$$h^+ + H_2O(ads.) \rightarrow OH^-(ads.) + H^+ \quad (15)$$

$$h^+ + OH^-(ads.) \rightarrow HO^\bullet(ads.) \quad (16)$$

$$HO^\bullet(ads.) + P(ads.) \rightarrow P_{ox}(ads.) \quad (17)$$

$$h^+ + P(ads.) \rightarrow P_{ox}(ads.) \quad (18)$$

Therefore, there coexist two parallel oxidation reactions in the UV/$TiO_2$ system: direct photolysis by UV irradiation, and free radical oxidation due to the hydroxyl radicals generated as in Eq. (16).

Fig. 1 shows the disappearance curves of azo dye in this group of experiments. It can be seen that there is an obvious divergence between the UV and vis photocatalysis. Table 1 lists the values of the global pseudo-first-order kinetic constants ($k$) and of the deduced radicalary path-way constants ($k_R$). According to Eq. (11) the value of $k_R$ can be calculated by the difference between the total decolourization value and the value of the photolytic path-way ($k - k_P$). The experimentally calculated $k_P$ values were $1.70 \times 10^{-3}$ $min^{-1}$ (for UV systems) and 0 (for vis-systems).

On the other hand, RR is a global approach to quantify the importance of the radicalary path-way regarding the global oxidation process. It is calculated as follows:

$$RR = \left[\frac{k_R}{k}\right] \times 100 \quad (19)$$

Table 1 also shows the colour removal at 15 min and the mineralization attained at 2 h (measured by COD and TOC removals). The parameter $\varepsilon_c^0$ is the oxidation state of the residual organic carbon and can be evaluated as follows:

$$\varepsilon_c^0 = \left[4 - 4\frac{COD_f/32}{TOC_f/12}\right] \quad (20)$$

In the evaluation of the efficacy of an oxidation system, so important as TOC removal is the oxidation state of the remnant organic carbon. This parameter ranged between −2.0 (for the initial dissolution) to −0.4 and −0.2 (for $TiO_2$/UV and $TiO_2/H_2O_2$/UV). However, the maximum removal of TOC and COD was obtained by $TiO_2/S_2O_8^{2-}$/UV and $TiO_2/H_2O_2$/UV, respectively. The order of efficacy, considering the degree of decolourization at 15 min was as follows:

$$TiO_2/H_2O_2/vis = TiO_2/vis < TiO_2/UV < TiO_2/S_2O_8^{2-}/UV < TiO_2/H_2O_2/UV$$

### 3.2. Homogeneous photocatalysis: oxidation systems based on Fenton-type reactions

Fenton-type processes are known to be very effective in the removal of many hazardous organic pollutants from water. The main advantage is the complete destruction of contaminants to harmless compounds, e.g. $CO_2$, water and inorganic salts. Fenton reagent's causes the dissociation of the oxidant and the formation of highly reactive hydroxyl radicals that attack and destroy the organic pollutants.

Table 2 lists the values of the pseudo-first-order kinetic rate constant, COD and TOC removals obtained at 2 h for each oxidation system. Considering the degree of dye decolourization at 15 min, the order of reactivity is as follows:

$$H_2O_2 = vis < H_2O_2/Fe^{3+}/vis < UV < UV/S_2O_8^{2-} < H_2O_2/Fe^{3+}/C_2O_4^{2-}/vis < H_2O_2/UV < H_2O_2/Fe^{3+}/UV$$

As can be seen in Table 2, the photo-assisted Fenton's system with light in the near-UV region, is especially powerful and leads to extensive mineralization of the azo dye (36% TOC removal, 48% COD removal). Its advantages over other advanced oxidation processes have been discussed [22]. The synergic effect observed for the combined photo-assisted Fenton's reagent system with respect to the sum of the two systems (Fenton's reagent + UV radiation) has recently been demonstrated [23].

The UV/visible irradiation accelerates ($H_2O_2/Fe^{2+}$) reactions, improving the degradation rates of organic pollutants, such as pesticides, dyes [24], chlorophenols, nitrogenated organic compounds, etc. This enhancement has been explained as due to $Fe^{3+}$-photocatalyzed reactions, i.e. photolysis of hydroxide complexes of $Fe^{3+}$ yielding hydroxyl radicals and regenerating $Fe^{2+}$ (Eq. (24)) and photochemical reactions of complexes formed between $Fe^{3+}$ and the organic substrate or its degradation intermediates (Eq. (25)), especially organic acids:

$$Fe^{2+} + H_2O_2 \rightarrow Fe^{3+} + HO^\bullet + OH^- \quad (21)$$

$$Fe^{3+} + H_2O_2 \rightarrow Fe(HO_2)^{2+} + H^+ \quad (22)$$

$$Fe(HO_2)^{2+} \rightarrow Fe^{2+} + HO_2^\bullet \quad (23)$$

$$Fe(OH)^{2+} \xrightarrow{h\nu} Fe^{2+} + HO^\bullet \quad (24)$$

Table 2
Rate constants and mineralization obtained at 2 h. Homogeneous photocatalysis

| System | Colour removal at 15 min (%) | $k \times 100$ ($min^{-1}$) | $k_R \times 100$ ($min^{-1}$) | RR (%) | COD removal[a] (%) | TOC removal[a] (%) | $\varepsilon_c^0$ |
|---|---|---|---|---|---|---|---|
| vis | 0 | 0 | 0 | 0 | 0 | 0 | −1.9 |
| UV | 3 | 0.17 | 0 | 0 | 0–5 | 0–5 | −1.9 |
| $H_2O_2$ | 0 | 0 | 0 | 0 | 0 | 0 | −1.9 |
| UV/$S_2O_8^{2-}$ | 8 | 0.46 | 0.29 | 63 | 12 | 13 | −1.9 |
| UV/$H_2O_2$ | 16 | 1.11 | 0.94 | 84 | 17 | 12 | −1.5 |
| $H_2O_2$/$Fe^{3+}$/vis | 1.3 | 0.02 | 0.02 | 100 | 0–5 | 0–5 | −1.9 |
| $H_2O_2$/$Fe^{3+}$/UV | 42 | 1.60 | 1.43 | 89 | 48 | 36 | −0.8 |
| $H_2O_2$/$Fe^{3+}$/$C_2O_4^{2-}$/vis | 8 | 0.40 | 0.40 | 100 | 23 | 4 | −1.8 |

Oxidation systems based on Fenton-type reactions. $\varepsilon_c^0$: final oxidation state of residual carbon.
[a] Results obtained at 2 h of reaction.

$$Fe^{3+}\text{-L} \xrightarrow[(L=\ RCOO^-)]{h\nu} Fe^{2+} + L^{\bullet} \quad (25)$$

The photo-assisted Fenton's reagent systems perform better than the UV/$H_2O_2$ system (see TOC, COD and colour removal) because $H_2O_2$ has a low molar extinction coefficient in the UV region (e.g. $\varepsilon$ = 19.61 l/(mol cm) at 254 nm), rendering it susceptible to inner-filter effects from absorbing compounds in solution. Also, $H_2O_2$ does not absorb at all above ~320 nm. A related method of producing $HO^{\bullet}$ from $H_2O_2$ is via Fenton's reagent (Eq. (21)). Fenton's reagent can be made catalytic by photoreducing the $Fe^{3+}$ ion in the near UV region (Eqs. (24) and (25)). The $Fe(OH)^{2+}$ ion absorbs light at wavelengths up to about 410 nm. Hence, the reaction can be carried out efficiently with longer wavelength light than other AOPs such as $O_3$/UV or $H_2O_2$/UV, which require wavelengths below ~300 nm [25].

However, as can be seen in Table 2, photo-Fenton process was very effective with UV irradiation, but shows to be little effective under vis-irradiation. This problem was resolved with the addition of oxalate anion, leading to an additional improvement of the photocatalytic efficiency. The $H_2O_2$/$Fe^{3+}$/$C_2O_4^{2-}$/vis process provides advantages, since ferrioxalate has a high molar absorption coefficient for longer wavelengths (up to 500 nm) and generates hydroxyl radicals with a high quantum yield. Other carboxylate and polycarboxylate complexes of $Fe^{3+}$ may not have spectral characteristics similar to those of ferrioxalate, and generally have much lower and wavelength dependent quantum yields as compared to ferrioxalate. The quantum yield of $Fe^{2+}$ formation in reaction (25) varies with different carboxylate ligands. The ferrioxalate complex is the best known and most widely studied.

$$Fe(C_2O_4)_3^{3-} + h\nu \rightarrow Fe^{2+} + 2C_2O_4^{2-} + C_2O_4^{\bullet -} \quad (26)$$

$$C_2O_4^{\bullet -} + Fe(C_2O_4)_3^{3-} \rightarrow Fe^{2+} + 3C_2O_4^{2-} + 2CO_2 \quad (27)$$

$$C_2O_4^{\bullet -} \rightarrow CO_2 + CO_2^{\bullet -} \quad (28)$$

$$C_2O_4^{\bullet -} \text{or} CO_2^{\bullet -} + O_2 \rightarrow 2\text{or}1CO_2 + O_2^{\bullet -} \quad (29)$$

The theoretical quantum yield for $Fe^{2+}$ generation is 2.0, but reaction (29) and the reverse of reaction (26) reduce this quantum yield. The measured quantum yield of $Fe^{2+}$ formation is about 1.0 from 250 to 450 nm and decreases with further increase of the irradiation wavelength. In air saturated solution, the intermediate oxalate radical reacts with molecular oxygen and generates the hydroperoxyl radical, which disproportionates to form hydrogen peroxide. The ferrous ion formed in reactions (26) and (27) can react with $H_2O_2$ present in solution and generate hydroxyl radicals (reaction (21)). Thus, the photolysis of ferrioxalate in the presence hydrogen peroxide provides a continuous source of Fenton's reagent.

### 3.3. Ozonation

The investigations deal with the light-induced decomposition of ozone in aqueous solutions [26,27] reveal a two-step process involving the light-induced homolysis of $O_3$ and the subsequent production of $HO^{\bullet}$ radicals by the reaction of $O(^1D)$ with water (Eqs. (30) and (31)) [28]:

$$O_3 + \lambda\nu < 310\text{nm} \rightarrow O_2 + O(1D) \quad (30)$$

$$O(1D) + H_2O \rightarrow HO^{\bullet} + HO^{\bullet} \quad (31)$$

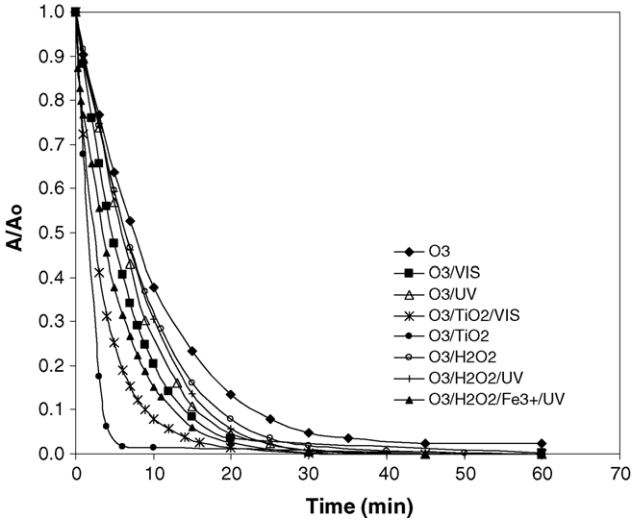


Fig. 2. Disappearance curves of dye in the group of experiments based on ozone.

Table 3
Rate constants and mineralization obtained at 1 h

| System | Colour removal at 15 min (%) | $k \times 100$ ($min^{-1}$) | $k_R \times 100$ ($min^{-1}$) | RR (%) | COD removal[a] (%) | TOC removal[a] (%) | $\varepsilon_c^0$ |
|---|---|---|---|---|---|---|---|
| $O_3$ | 77 | 10.2 | 10.2 | 100 | 44 | 10 | +0.4 |
| $O_3$/vis | 92 | 16.9 | 16.9 | 100 | 59 | 38 | +0.2 |
| $O_3$/UV | 89 | 15.5 | 15.3 | 99 | 66 | 43 | +0.5 |
| $O_3/H_2O_2$ | 84 | 12.4 | 12.4 | 100 | 57 | 36 | +0.1 |
| $O_3/TiO_2$ | 99 | 70.0 | 70.0 | 100 | 67 | 45 | +0.5 |
| $O_3/H_2O_2$/UV | 86 | 15.8 | 15.6 | 99 | 70 | 50 | +0.5 |
| $O_3/TiO_2$/vis | 97 | 25.0 | 25.0 | 100 | 58 | 41 | −0.2 |
| $O_3/H_2O_2$/UV/$Fe^{3+}$ | 95 | 17.9 | 17.7 | 99 | 82 | 60 | +1.4 |

Ozonation. $\varepsilon_c^0$: final oxidation state of residual carbon.
[a] Results obtained at 1 h.

$$O_3 + H_2O + \lambda\nu \rightarrow H_2O_2 + O_2 \quad (32)$$

However, it has been observed that photolysis of ozone dissolved in water leads to the production of hydrogen peroxide (Eq. (32)) in a sequence of reactions, where hydroxyl radicals, if formed at all, do not escape from the solvent cage. It has been proved that hydrogen peroxide is in fact the primary product of ozone photolysis.

The authors suggest that initiation can occur by the reaction of ozone with $HO^-$ or $HO_2^-$, or by photolysis of hydrogen peroxide. The latter is formed by ozone photolysis as well as from the reaction of ozone with many unsaturated organic compounds. $HO^\bullet$ radicals react with organic substrates to produce organic radicals, which efficiently add molecular oxygen to yield organic peroxyl radicals. These peroxyl radicals may be considered as the true propagators of the thermal chain reactions of oxidative substrate degradation and oxidant consumption.

Fig. 2 shows the disappearance curves of dye in the group of experiments based on the application of ozone. Taking as reference the level of decolourization attained at 15 min, the different processes were ranked in terms of efficacy as follows:

$$O_3 < O_3/H_2O_2 < O_3/H_2O_2/UV < O_3/UV = O_3/vis < O_3/H_2O_2/UV/Fe^{3+} < O_3/TiO_2/vis < O_3/TiO_2.$$

Table 3 lists the values of the pseudo-first-order kinetic rate constant, COD and TOC removals obtained at 1 h. Comparing Tables 1–3, and taking into account; the kinetic rate, the mineralization attained and the oxidation state of remnant organic carbon; we can assure that the processes that use ozone obtain better results. COD removals ranged between 44% (ozone) and 82% (for ozone-photo-Fenton) and the oxidation state of residual organic carbon is positive for all cases.

As can be seen, ozone-photo-Fenton system leads to a TOC and COD removal of 60% and 82%, respectively. This system leads to the greater oxidation state of remnant organic carbon ($\varepsilon_c^0 = +1.4$). The colour removal obtained at 15 min was 95% and the pseudo-first-order constant was 17.9 $min^{-1}$, 100 times faster than the single UV process.

Once it is found that the addition of vis or $H_2O_2$ by themselves exerts no oxidizing activity against azo dye (see Table 2), it can be deduced that the addition of these agents has a slight synergic or catalytic effect on the oxidant activity of ozone (see Table 3), presumably due to free radical generation. On the other hand, the synergic effect of the addition of ozone to the photo-Fenton's reagent system is very high ($k$ value is 10 times greater). This synergic effect can also be observed in the ternary process UV/$H_2O_2$/$O_3$, which is not equal to the sum of the binary UV/$H_2O_2$ process plus the simple process $O_3$. Neither it is equal to the sum of the three individual processes, so that there is a clear synergy involved. This synergy is the reason behind the recent trend towards using combinations of different oxidants. Nevertheless, taking into account the colour removal at 15 min, the faster oxidation system is $O_3/TiO_2$.

Taking into account that the treatment of a waste stream does not necessarily require total mineralization of the organic pollutant, rather the disappearance and partial oxidation of the pollutant may be sufficient. In this case the $O_3/TiO_2$ process can be considered the more interesting. The colour removal at 15 min was 99% and the pseudo-first-order constant was 70.0 $min^{-1}$, four times faster than the $O_3/H_2O_2$/UV/$Fe^{3+}$ process and without light costs. The literature examined [29] indicates that ozone can be adsorbed on a catalyst surface to yield different species (Eqs. (33) and (34)) [30]. Moreover, azo dye can be adsorbed on the catalyst surface (Eq. (35)) and a surface reaction can be considered between both adsorbed species (Eq. (36)). The reaction mechanism can be represented by the following steps:

$$O_3 + S \rightleftarrows O_3{-}S \quad (33)$$

$$O_3{-}S \rightarrow O{-}S + O_2 \quad (34)$$

$$P + S \leftrightarrows P{-}S \quad (35)$$

$$O{-}S + P{-}S \leftrightarrows P_{ox} + 2S \quad (36)$$

where S represents the free active centers at the catalyst surface, and P the azo dye.

## 4. Conclusions

In this work, degradation of Acid Red 88 azo dye in water was investigated using 21 oxidation processes. Colour, COD and TOC removals were evaluated for each oxidation system. The major findings include:

The order of efficacy, considering the degree of decolourization at 15 min, is as follows: $H_2O_2$ = vis < $H_2O_2/Fe^{3+}$/vis < $TiO_2/H_2O_2$/vis = $TiO_2$/vis < UV < UV/$S_2O_8^{2-}$ < $H_2O_2/Fe^{3+}/C_2O_4^{2-}$/vis < $H_2O_2$/UV < $H_2O_2/Fe^{3+}$/UV < $TiO_2/S_2O_8^{2-}$/UV < $TiO_2$/UV = $TiO_2/H_2O_2$/UV < $O_3$ < $O_3/H_2O_2$ < $O_3/H_2O_2$/UV < $O_3$/UV = $O_3$/vis < $O_3/H_2O_2$/UV/$Fe^{3+}$ < $O_3/TiO_2$/vis < $O_3/TiO_2$.

In general, the processes that use ozone obtain better results. Removals of COD ranged between 44% and 82%, TOC 10–60% and colour, 77–99% (at 15 min). Notice that ozone-photo-Fenton system leads to a maximum TOC and COD removal (60% and 82%, respectively). However, taking into account the colour removal, $O_3/TiO_2$ process can be considered the more interesting system (95% of decolourization at 3 min).

On the other hand, photo-assisted Fenton system with light in the near-UV region is especially powerful (48% of COD removal) but shows to be little effective under vis irradiation (0–5% of COD removal). This problem can be reduced with the addition of oxalate anion, leading to an additional improvement of the photocatalytic efficiency (23% of COD removal).

In the case of heterogeneous photocatalysis using titanium dioxide, $TiO_2/H_2O_2$/UV process obtain better results for colour and COD removal, nevertheless, $TiO_2/S_2O_8^{2-}$/UV leads to the greatest TOC removal.

## Acknowledgements

This research was supported by the Comision Interministerial de Ciencia y Tecnología (CICYT) under Project CTQ 2004-00961/PPQ, and by the Junta de Extremadura under Project 2PR01A113.

## References

[1] I. Arslan, J. Hazardous Mater. B 85 (2001) 229.
[2] P.C. Vandevivere, R. Bianchi, W. Verstraete, J. Chem. Technol. Biotechnol. 72 (1998) 289.
[3] C. Galindo, P. Jacques, A. Kalt, J. Photochem. Photobiol. A: Chem. 141 (2001) 47.
[4] O. Legrini, E. Oliveros, A.M. Braun, Chem. Rev. 93 (1993) 671.
[5] M. Neamtu, A. Yedilerb, I. Siminiceanua, M. Macoveanua, A. Kettrupb, Dyes Pigments 60 (2004) 61.
[6] R.G. Rice, M.E. Browning, Industrial Wastewater, Noyes Data Corp., Oark Ridge, NJ, 1981.
[7] S.J. Masten, H.R. Davies, in: J.O. Nriagen, M.S. Simmons (Eds.), Environmental Oxidants, Wiley, New York, 1993.
[8] I. Arslan, A. Balcioglu, T. Tuhkanen, Environ. Technol. 20 (1999) 921.
[9] J. Staehelin, J. Hoigné, Environ. Sci. Technol. 16 (1982) 676.
[10] B. Legube, N.K.V. Leitner, Catal. Today 53 (1999) 61.
[11] J. Beltran, F.J. Rivas, R. Montero-de-Espinosa, Appl. Catal. B: Environ. 47 (2004) 101.
[12] C. Nasr, K. Vinodgopal, L. Fisher, S. Hotchandani, A.K. Chattopadhyay, P.V. Kamat, J. Phys. Chem. 100 (1996) 8436.
[13] R.W. Matthews, Water Res. 25 (1991) 1169.
[14] J. Zhao, K. Wu, T. Wu, H. Hidaka, N. Serpone, J. Chem. Soc., Faraday Trans. 94 (1998) 673.
[15] K. Vinodgopal, D.E. Wynkoop, P.V. Kamat, Environ. Sci. Technol. 30 (1996) 1660.
[16] F. Zhang, J. Zhao, T. Shen, H. Hidaka, E. Pelizzetti, N. Serpone, Appl. Catal. B: Environ. 15 (1998) 147.
[17] R.F.P. Nogueira, W.F. Jardim, J. Chem. Edu. 70 (1993) 861.
[18] J. Beltrán, J.R. Domínguez, R. López, J. Chem. Technol. Biotechnol. 79 (2004) 407.
[19] I.A. Alaton, I.K. Balcioglu, D.W. Bahnemann, Water Res. 36 (2002) 1143.
[20] A. Topalov, D. Molnár-Gábor, J. Csanádi, Water Res. 33 (1999) 1371.
[21] C. Turchi, D. Ollis, J. Catal. 122 (1990) 178.
[22] G. Ruppert, R. Bauer, G. Heisler, Chemosphere 28 (1994) 1447.
[23] S.M. Kim, A. Vogelpohl, Chem. Eng. Technol. 21 (1998) 187.
[24] F. Herrera, J. Kiwi, A. Lopez, V. Nadtochenko, Environ. Sci. Technol. 33 (1999) 3145.
[25] P.L. Huston, J.J. Pignatello, Water Res. 33 (1999) 1238.
[26] G.R. Peyton, F.Y. Huang, J.L. Burleson, W.H. Glaze, Environ. Sci. Technol. 16 (1982) 448.
[27] W.H. Glaze, G.R. Peyton, S. Lin, F.Y. Huang, J.L. Burleson, Environ. Sci. Technol. 16 (1987) 454.
[28] W.H. Glaze, J.W. Kang, D.H. Chapin, Ozone Sci. Eng. 9 (1987) 335.
[29] J. Beltran, F.J. Rivas, R. Montero-de-Espinosa, Appl. Catal. B: Environ. 39 (2002) 221.
[30] B. Dhandapani, S.T. Oyama, Appl. Catal. B: Environ. 11 (1997) 129.